www.maajournal.com

Mediterranean Archaeology and Archaeometry
Vol. 21, No 2, (2021), pp. 37-67
Open Access. Online & Print.

DOI: 10.5281/zenodo.4643739

THE MORTARS FROM ROCK-CUT HYDRAULIC STRUCTURES OF AS-SILA (SELA) IN SOUTHERN JORDAN: MINERALOGICAL CHARACTERIZATION AND RADIOCARBON DATING

Rocío Da Riva[1*], Francisco Javier Santos Arévalo[2], and Marisol Madrid i Fernández[1]

[1]Departament d'Història i Arqueologia, Universitat de Barcelona, GRACPE research team, Spain
[2]Centro Nacional de Aceleradores (Universidad de Sevilla, CSIC, Junta de Andalucía), Spain

Received: 26/12/2020
Accepted: 27/03/2021

**Corresponding author: Rocío Da Riva (mrdarivam@ub.edu)*

ABSTRACT

One of the aims of the 2016 campaign in as-Sila was to conduct a survey in order to identify cisterns, channels and structures related to water use at the top of the settlement, using the 2015 survey map of the site as a base. The investigations have revealed a complex and sophisticated hydrological network with a great diversity of water structures (carved in the sandstone and designed for the collection, storage, transport and distribution of rainwater). All the structures have been identified and described using a total station, their location associated with the general topography of the site, and the contexts photographed. This study presents the results of recent analyses of lime-based mortars from rock-cut hydraulic structures collected during the 2016 archaeological campaign at the site of as-Sila/Sela, in the governorate of Tafilah in southern Jordan. Mineralogical and petrographic analyses were performed on 16 samples of mortars by means of x ray diffraction (XRD) and thin-section petrography (OM), and 12 AMS radiocarbon dates were taken from them. In spite of the difficulties in dating lime-based mortars and the problems inherent in the interpretation of the data, here we present the most complete analysis currently available of mortars from an archaeological site in southern Transjordan.

KEYWORDS: mortars, hydraulic structures, Transjordan, hilltop settlements, mineralogical analyses, thin-section petrography, AMS radiocarbon analyses

1. INTRODUCTION AND OBJECTIVES

The site of as-Sila is located in the northern Edomite Plateau, west of the Wadi Arabah, very close to modern-day Busayra in southern Jordan (Fig. 1). The site stands on a rocky promontory 200 m above the surrounding wadis. Sela was an important centre in the Late Iron Age (1000-539 BCE)[1], as the presence of remains from this period testifies – among them, the impressive Neo-Babylonian monument of King Nabonidus (556–539 BCE) with a relief representing the king and the remains of a cuneiform inscription (MacDonald, 2004, Site 134; Da Riva, 2019; Da Riva, 2020)[2]. Modern-day as-Sila is one of the sites potentially identified with Sela of the Hebrew Bible, but this identification is uncertain. The relative chronology of the surface material (pottery) confirms occupation during at least the Late Iron Age, the Nabataean/Roman, Ayyubid, Mamluk and Ottoman periods. The cuneiform inscription of Nabonidus provides an independent date in the Late Iron Age, and the results of the 14C analysis of timber recovered from a building excavated in area F of the promontory (House 1, see Da Riva et. al., forthcoming) provide absolute chronologies for occupation in the Mamluk and Ottoman periods.

The research work carried out at Sela since 2015 has revealed a large-scale site of approximately 43 ha, with a considerable number of architectural structures of different periods, sizes, morphologies and, presumably, functions: rock-cut houses, remains of large buildings, towers, and so on. The most notable feature of the site, however, is the presence of water structures: channels, tanks, rock-cut water cisterns and other structures used for rainwater harvesting and its storage, transport and management (Shqiarat Mansour 2019). More than a hundred of these structures have been documented in the course of the surveys, making Sela an ideal and unique site to study water management in the highlands of southern Jordan[3].

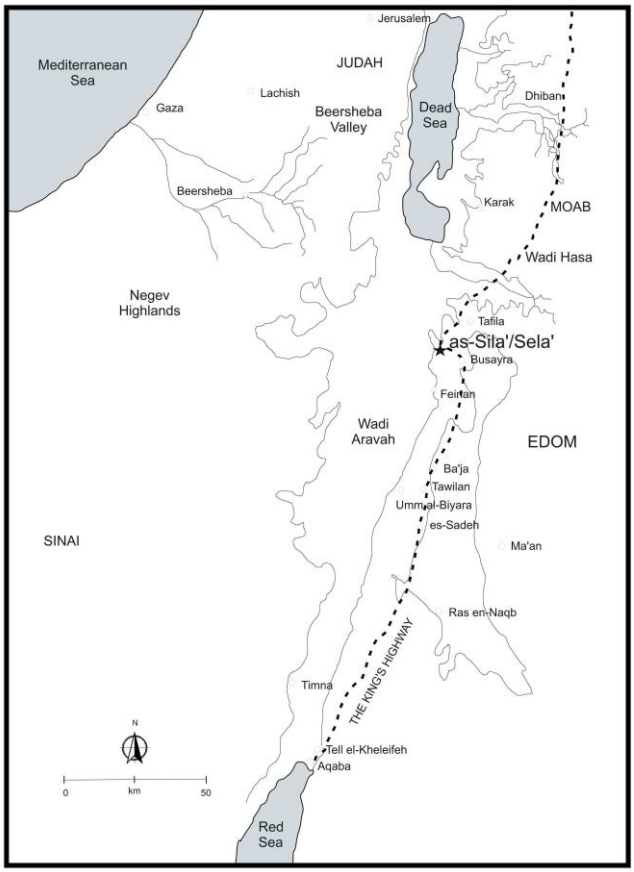

Figure 1. Map of Jordan showing the location of Sela (after Porter, 2004, 375)

During our first campaign (2015) we undertook a survey of the site and produced a cartographic base for future studies (Fig. 2). The work was carried out using case studies in the area, mostly in the vicinity of Busayra, and archaeological data and charts stored in the JADIS (Jordan Antiquities Database and Information System) – MEGA (Middle Eastern Geodatabase for Antiquities) of the Department of Antiquities and Tourism in Jordan. The archaeological field survey of 2015 was non-intrusive and extensive (Da Riva et. al., 2017). Given the size of the site (42,0089 ha), in order to facilitate the surveys and the fieldwork, in 2015 we decided to divide the surface in a series of areas, indicated by the letters A-L on the sketch map (Fig. 3).

[1] Here we follow Bienkowski's chronology for Edom (MacDonald, 2015, 24).

[2] Water management in Sela presents parallels with other settlements in the area, such as Ba'ja III, Umm al-Biyara, Jabal al-Qseir, etc. (Lindner, 1992). A study of the water structures in Sela is the object of an ongoing thesis at the University of Barcelona by R. Marsal under the supervision of R. Da Riva and J. C. Moreno-García.

[3] All the information gathered by the project has been placed at the disposal of the Department of Antiquities of Jordan (DoAJ) of the Ministry of Tourism and Antiquities in the form of reports and site cards to be included in the Middle Eastern Geodatabase for Antiquities (MEGA) Jordan database: http://megajordan.org.

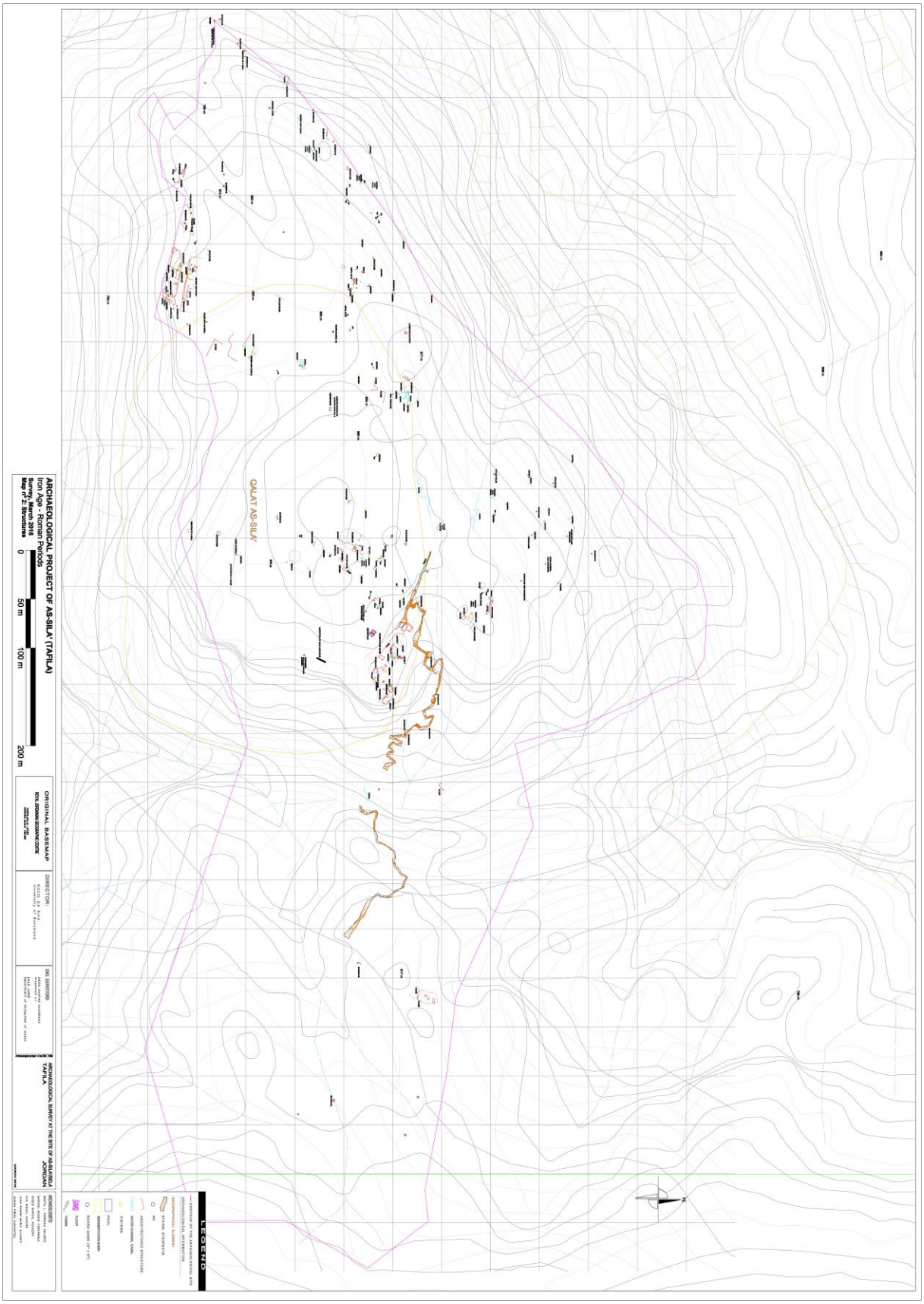

Figure 2. Cartographic plan of Sela with the structures documented in the course of 2015 and 2016 surveys (by E. Jariri, D. Gaspar and J. Muñiz,)

One of the main features of the 2016 campaign was the survey conducted to identify cisterns, channels and structures related to water use at the top of the mountain of as-Sila, using the 2015 survey map of as-Sila as a base. All the structures were identified and described in the course of the 2015 and 2016 archaeological surveys with a total station, they were individually labeled, contextualized in the different areas of the site, and linked with the architectural arrangements. We also associated the location of the water structures with the topography and geology of the site so as to identify the general hydrological network.

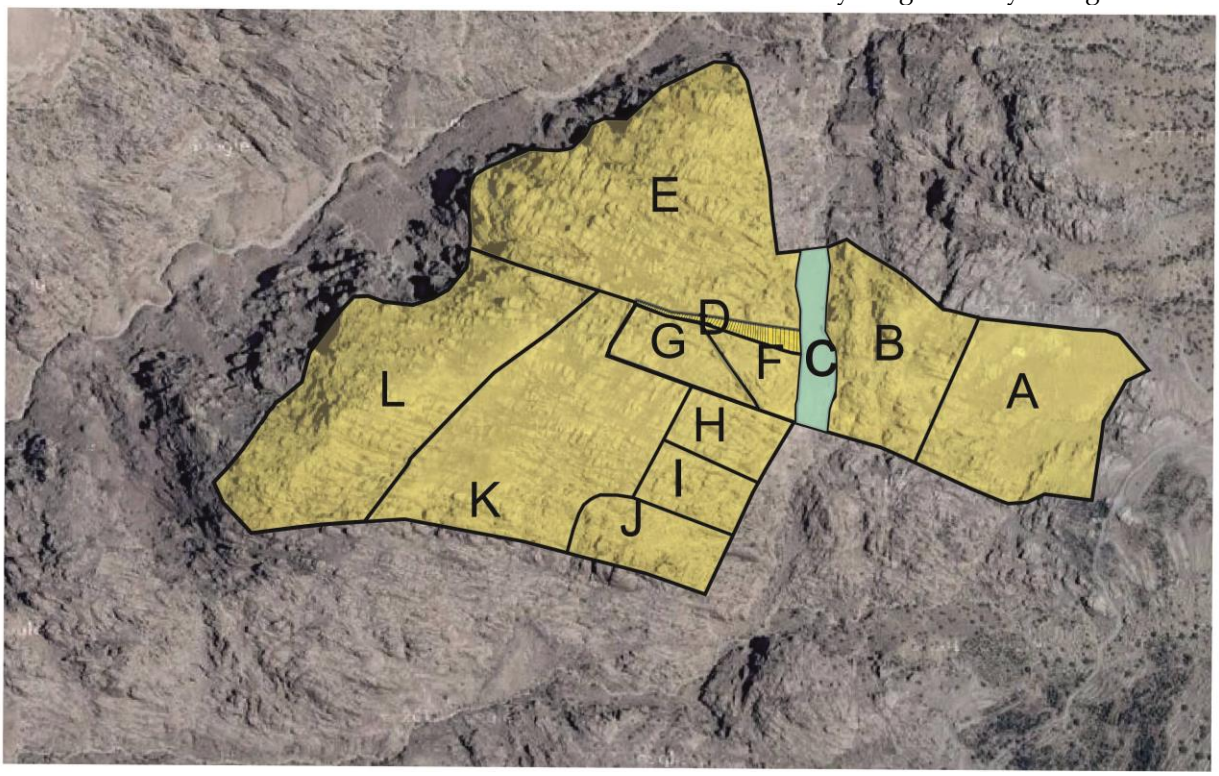

Figure 3. Sketch map of Sela (by R. Marsal after Corona Atlas & Referencing System, http://corona.cast.uark.edu/)

In the course of the last campaign in Sela in the autumn of 2018, the Sela team studied the cuneiform inscription of Nabonidus with the assistance of professional climbers. The aim of this campaign was to elucidate the archaeological context of the monument and, later, to create a 3D model of it. Some of the water structures were studied at the same time, and archaeologists and pottery specialists undertook a detailed survey of the whole site, both on top of the promontory as well as in the eastern side of the wadi, collecting sherds for analysis (Da Riva, 2020).

During the 2015, 2016 and 2018 campaigns, the water structures of Sela were identified and their contexts photographed, but as they were not excavated, no typology could be established. However, a thorough investigation of the mortars of some cisterns was carried out in order to complement the information obtained from the direct field study carried out in the structures of Sela. The main objectives of this investigation were: a) to observe whether the diversity of the cisterns was in line with the variety in the production of the mortars that protect and waterproof the hydraulic structures; and b) to date them in order to contextualize the use of the cisterns within a certain period of time.

With these objectives in mind, during the archaeological campaign carried out at the site in the spring of 2016, a sample of 16 mortars associated with hydraulic structures and residential areas were selected for archaeometric study (Da Riva et al., forthcoming). Mineralogical characterization by means of XRD and petrographic analysis were performed, and finally some of the mortars were selected for radiocarbon dating. In order to avoid bias, the mortar samples were taken randomly; that is, there was no prior selection of the cisterns from which they were taken.

2. SELA: SETTLEMENT AND CHRONOLOGY

Although surface finds and excavations at the summit indicate that as-Sila/Sela was occupied during several periods (at least the Iron Age and the Nabataean, Mamluk and Ottoman periods), the site's most extensive occupation and use were during I millennium BCE, in the Iron Age II period, the time of the Biblical Edomites and the Neo-Assyrian and Neo-Babylonian empires. In fact, Sela is one of the so-called "hilltop settlements", a type of mountain site that flourished in the region in the Late Iron Age (Ben David, 2015), and there are indications of pottery and

architectural structures comparable to those found at other nearby Iron Age II sites, such as Umm al-Biyara, Busayra, Hesban, Ba'ja and Umm el-Ala (Lindner and Farajat, 1987; Lindner, 1992). Indeed, the study of the surface pottery carried out by archaeologists Najjar and Herles in 2018 revealed a variety of periods and a broad chronological framework, which bears witness to the long-term occupation of the settlement. Interestingly, no Bronze Age or Iron Age I pottery was found in the course of the survey, although of course an ephemeral occupation of the site in those periods, or even earlier, cannot be ruled out. The extent and continuity of these occupations is difficult to estimate at this stage in the research, but the many structures related to rainwater harvesting and storage documented during the surveys suggest that the occupation was intense, at least for certain periods. All this evidence suggests that the beginning of the permanent settlement of Sela dates from Iron Age II, when the techniques of water management (catchment, distribution and storage) were mastered. Accordingly, Sela was only habitable on a stable basis if water was properly managed, and this was only possible by means of the construction of water channels, reservoirs and cisterns. The available evidence suggests that water management in Sela began during the Late Iron Age and continued until the Ottoman period.

3. THE HYDRAULIC STRUCTURES OF SELA

A notable feature of Sela is the presence of approximately a hundred cisterns, water reservoirs perforated or carved into the sandstone, presumably filled with rainwater through surface channels incised in the rock. These cisterns are exceptional for their variety; some of them are carved into the sandstone in the ground, and others are cut into the standing sandstone boulders. The shapes and sizes vary, as does the level of sophistication: some are technologically complex, with settling or sedimentation basins for stopping sediment and for separating mud and sand before the water was allowed into the main cisterns (Fig. 4).

Figure 4. House with canals, sedimentation basin and cistern D15

Some cisterns are more or less oval in shape; others are rounded, and others still are rectangular or square, with corners forming right angles. Some have plaster or water-proof mortar on their sides and/or a

slab of stone to close them; these additions would have helped to improve the quality of the water, lengthen the potential storage time, and reduce the loss of water through evaporation. It is plausible to think that the structures were reused over time, and that mortars were added during different periods of use; so a cistern may have been manufactured in one particular period, but the mortar currently present in it may be more recent. The variability in size and morphology of the cisterns may respond to chronological differences. We assume that different artisans in different periods used different technologies and elements to manufacture the cisterns and their mortars, which implies that the system was used in more than one period. However, we did not attempt to establish an accurate and definitive typology of the structures because of the difficulty in obtaining a 14C-dating and the lack of independent archaeological evidence. Most of these cisterns are now filled with debris and sediment, so there is no way of dating or analysing them without undertaking an archaeological excavation. In some of them a preliminary inspection was performed using a Kong Cevedale tripod (Fig. 5). In addition to the cisterns, a series of rock-cut channels and pipelines were detected in different areas of the site. Some of the channels are more than 20 m in length, and they seem to have been used to funnel the water into the cisterns. All these elements suggest the existence of an extremely sophisticated and well-developed system for harvesting and storing rainwater using water channels, pipes, pools, and underground cisterns.

Figure 5. Studying cistern D18 in September 2018

Water structures have been documented in the promontory of as-Sila as well as in the wadi area below (areas A and B in Fig. 3 above). The samples from the analysis published here were obtained in the course of the 2016 campaign in areas F, G, H, K and L. Areas F, G and H are located to the north and east of the site, near the monumental entrance to the summit, while areas K and L lie to the south and southwest respectively. Structures D13 and D115 are located in area F. The entrance area (F) includes a monumental gate, a hollow tower (perhaps a cistern, or maybe a silo, identified as D10, see Fig. 28 below), and some "houses" with stone-walls (Lindner et al., 2001, 252-258). The gate is rock-cut, with a reinforcement of stone ashlars to build the walls. D01 (Fig. 6), D03 (Fig. 7), D05, (Fig. 8), D09 (Fig. 9), D16 (Fig. 10) and D63 are

from area G. In area G we found the rock-cut layout of a large structure, some houses and cisterns. D22 (Fig. 11) and D107 are from area H. This area presents two large rock-cut structures, one of which at least seems to have functioned as a sanctuary: there is an altar and a sort of sacrificial pile or baytilos (Lindner et al., 2001, 263). D38 (Fig. 12) is from area K. The central area K is the largest at the site; here, we found numerous cisterns, rock-cut houses and also a canal. Surface finds (pottery, stone and metal objects) coincide with those of other areas of the site. D57 and D59 are from area L. In this western part, we found a tower and some rock-cut structures, including houses and cisterns. We also detected a limestone outcrop, which was probably the quarry for the plaster used for the walls and floors of the cisterns and the houses. Near the limestone outcrop, we found iron slags and some fragments of basalt objects.

Figure 6. Cistern D01

Figure 7. Cistern D03

Figure 8. Cistern D05

The observations below regarding the morphology of the cisterns are preliminary; a detailed study could not be carried out, as most of the cisterns were filled with sand, debris and/or vegetation, and none of the structures were excavated. D01, D05, D22 and D63 lack a regular shape; the cisterns are completely filled so they could not be studied or measured. D03 and D09 are both oval in shape; D03 is not silted, and

they were both inspected in September 2018. D13 is filled with some vegetation and debris; it has a circular opening and four canals are connected with it. These canals are covered with rectangular sandstone slabs. The canals and the cistern were inspected using a tripod in September 2018 (Fig. 13). D16 is partially filled; it is nearly oval in shape, and it was inspected in 2018. Cisterns D38, D57 and D59 (filled) are also oval-shaped. D107 and D115 are indeterminate, but the presence of lime-based mortars points to their use as hydraulic structures, and so samples were taken from these two structures.

Figure 9. Cistern D09

Figure 10. Cistern D16

Figure 11. Cistern D22

Figure 12. Cistern D38

Figure 13. Documenting cistern D13 (R. Da Riva, A. Noriega, D. González) in September 2018

4. A BRIEF HISTORY OF THE USE OF MORTARS

The use of gypsum and lime mortars and/or plasters for building purposes was known in the Near East from prehistoric times. (Kingery, et al., 1998). The production of mortars or plasters has been described as a multi-phase, well-standardized process, and it is considered as the first invention ever made to alter the chemical composition of raw materials using pyrotechnology in the Eastern Mediterranean and Near East (Gourdin and Kingery, 1975). In this regard, the study of lime plasters and pottery from several sites in the region suggests that the burning of limestone may have been the direct predecessor of the firing of ceramics. Plasters or mortars, like pottery, are composite materials that possess a complex structure of different parts made out of assorted materials used for different purposes (Buxeda and Madrid, 2016). Also, like pottery, plasters vary in terms of their complexity depending on the intended final product, which might involve a range of raw materials (binder and aggregates).

On the basis of their physical condition and, most importantly, on the context in which the materials were used, a "plaster" could be any "mortar" or binder material used for wall and floor covering for smoothing, waterproofing, or preparing for paintings and decorations. In turn, a "mortar" could be a binder and small-sized aggregate material mostly used as a structural binder between masonry units such as bricks or stones (Hobbs and Siddall, 2011, 34-36; Artioli, et al., 2019, 159.).

The first step in this multi-phase process is the selection and collection of the raw materials. The best raw sources contain at least over 90% of calcium carbonate (Brysbaert, 2007), and in the case of Sela, the presence of quarries of limestone on the promontory (Fig. 14) would have allowed easy access to the raw material. The second step is the calcination process, which was probably carried out in proximity to the quarries, thus reducing transportation, effort, and costs. Considering the large number of water structures documented at Sela, a vast amount of fuel would have been necessary to process the limestone. Although timber is one of the best and most efficient combustibles, dung, peat, straw, or wood from shrubs could also have been used (Hauptmann and Ünsal, 2001).

After calcination, in the slaking process the quicklime is hydrated by adding water, forming slaked lime or lime putty, also called "portlandite" or calcium hydroxide ($Ca(OH)_2$). The resulting slaked lime is stored in slaking pits protected from any contact with air so as to avoid recarbonation. Although the ideal maturing time for the best quality lime putty is three or four years, the material may be sufficiently mature after only two weeks or a month.

The last step before putting the hydrated lime to use is to mix it with aggregates in order to increase the strength of the product and to enhance the drying rate; this minimizes the risk of shrinking and cracking of the plaster and increases the amount of plaster made from a given amount of slaked lime. Sand or ground limestones are the most frequently used aggregates (Brysbaert, 2007; Kingery, et al., 1998).

Finally, when the plaster is applied to a specific construction/structure, the paste of the hydrated lime putty dehydrates slowly in contact with the air and reacts with CO_2, producing a hard material composed of microcrystalline calcite, called secondary calcite. Chemically it is the same as the original raw material, primary calcite, but it has a different structure and a far smaller grain size (Brysbaert, 2007).

From a technical point of view, the quality of the binder depends on a variety of parameters including the composition, porosity and purity of the fired raw material, together with calcination, slaking and storing until the final paste for plastering is achieved. In this regard, the ideal raw material should be free of non-carbonated mineral content (silicates and clays) or < 5–10 wt. %, and the raw sources should be as pure as possible (i.e., murex, limestone) (Brysbaert, 2007). If the carbonate contains magnesium, derived from the presence of magnesian calcite or dolomite, then the material is a magnesian- or dolomitic-lime. The periclase (MgO) produced together with lime during calcination has much slower rehydration kinetics than CaO (Artioli, et al., 2019, 163). Besides, the mechanical properties of mortars may be improved by adding to the mixture organic materials such as egg white, recently identified by FTIR on some ancient mortars from Gerasa (Jordan) (Al Sekhaneh et al. 2020).

Figure 14. Limestone outcrop in area L. Photo by Robert Bewley APAAME 20181014 RHB-0373©APAAME

5. MATERIALS AND METHODS

The 16 samples taken from the hydraulic structures underwent petrographic and mineralogical analysis and 12 also underwent chronological analysis. The samples belong to water cisterns (D01*, D03, D05*, D09, D13, D16, D22, D38, D57, D59 and D63*), or to structures of undetermined function that may have been related to water management (D107 and SL'16.H1.UM3.1 and SL'16.H1.UM3.2 (from structure D115). Samples SL'16.H1.2.498* and SL'16.H1.6.169 were obtained from a house (H1) in area F (Table 1). The petrographic and mineralogical analyses were carried out at the *Laboratorio de Geoarqueología of the Institut Català de Paleoecologia Humana i Evolució Social* (IPHES) in Tarragona, and the study of the possible dating of the mortars at the *Centro Nacional de Aceleradores* (CNA) of the Universidad de Sevilla, Junta de Andalucía and CSIC in Seville.
(* = Samples not sent for radiocarbon dating at CNA).

5.1. *Mineralogical and Textural Characterization of the Mortars*[4]

For the petrographic examination, the samples were pre-consolidated by impregnation in resin under vacuum. Thin sections were then cut with oils to avoid damaging water-soluble minerals in the mortars and were polished to the standard thickness of 30 μm and covered with a glass slip. A petrographic microscope (Nikon Eclipse E40 POL, 20–400x) was used for the textural and mineralogical analyses, identification of aggregate materials and calculations of the binder/aggregate ratio, and assessment of the porosity of the mortars. Mineralogical characterization on thin sections was performed by means of μXRD with a Bruker-AXS D8 Discover diffractometer, in order to identify the main mineralogical phases of the mortars. Measurements were made using an EIGER2 R 500K Detector Hybrid Photon Counting. Measurements were taken from (5 to 70) °2θ. Evaluations of the crystalline phases present in each specimen analyzed were performed by using the DIFFRACT.SUITE software.

[4]This section is partially based on the report conducted by Soto (2017).

Table 1. Samples of mortars from Sela included in this study

Number of Sample	Sample	Area	Sector	Context	Structure	Reference of the structure
1	Mortar	F	-		Cistern	D13
2	Mortar	G	-		Cistern	D16
3	Mortar	G	-		Cistern	D63
4	Mortar	G	-		Cistern	D01
5	Mortar	G	-		Cistern	D03
6	Mortar	G	-		Cistern	D09
7	Mortar	G	-		Cistern	D05
8	Mortar	H	-		Cistern	D22
9	Mortar	G	-		Cistern	D38
10	Mortar	L	-		Cistern	D57
11	Mortar	L	-		Cistern	D59
13	Mortar	F	-		Undetermined	D107
1	Mortar	F	House 1	UM 3	Undetermined	D115
2	Mortar	F	House 1	UM 3	Undetermined	D115
169	Mortar	F	House 1	6	Undetermined	-
498	Mortar	F	House 1	2	Undetermined	-

The mineralogical and petrographic analyses suggest that all samples are lime-based plasters/mortars, showing variances in grain size, aggregates and proportions binder/aggregates that indicate different preparations or recipes. The textural and compositional study identified five different types, although categories 4 and 5 comprised only one sample each and should therefore be considered with caution. The results of the petrographic examination of most of the samples of type 1 (Fig. 15), show that the binder is defined as microsparitic calcite (1–10 μm), in proportions of 70–80% of the sample, and that the majority of aggregates are sub-rounded detrital quartz and microsparitic limestone, in amounts of 2–5% and 5–10% respectively. Those components would have been obtained from limestone (carbonate sedimentary rock) and sandstone (clastic sedimentary rock) in the surrounding area. Besides, the presence (not always combined) of fragments of crushed ceramics, ashes, plants and hematite, in varying proportions of between 1–2% of the total sample is occasionally observed. Crushed ceramics as an aggregate are found in Near Eastern sites in plasters/mortars related to water-bearing constructions where waterproofing is important: for instance, in Tell es-Safi/Gath (Israel), during the Iron Age (Regev et al., 2010); Petra, during the Nabataean period (Al-Aseer, 2000); or Sagalassos (Turkey), during the Roman and Hellenistic period (Degryse et al., 2002; Vázquez-Calvo et al., 2016; Benedetto et al., 2018) and later (Al Sekhaneh et al., 2020; Salama et al., 2017; Theologitis et al., 2021).

The systematic use of crushed ceramics in structures that required resistance to water (cisterns, aqueducts, fountains and baths) was frequent in Roman constructions from the beginning of the second century BCE onwards, giving rise to the popular opus signinum (Artioli, et al., 2019, 173; Pavia and Caro, 2008). The binder/aggregate ratio is 3/1, an optimal proportion: a ratio > 3/1 is likely to tend to shrinkage whilst a mixture with a ratio < 3/1 is liable to decompose because the binder is insufficient to hold all the components together (Pecchioni, et al., 2014). In addition, mineralogical analyses confirm the presence of calcite, quartz and dolomite as dominant minerals in the composition of this mortar (Fig. 16).

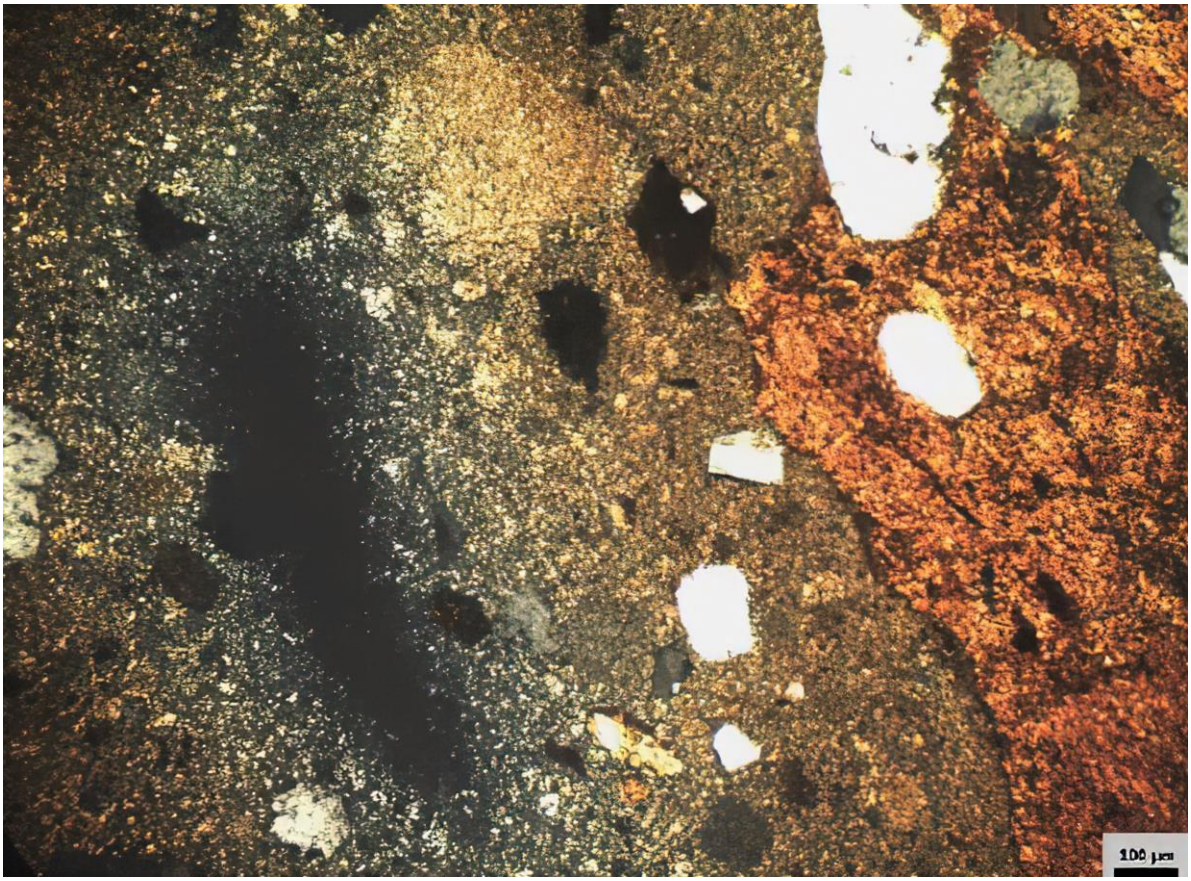

Figure 15. Optical micrograph of the thin section of lime mortar type 1. The image in plane polarized light shows fragments of detrital quartz as aggregate and the lime binder matrix (Soto, 2017, p. 13, fig. 2.2.)

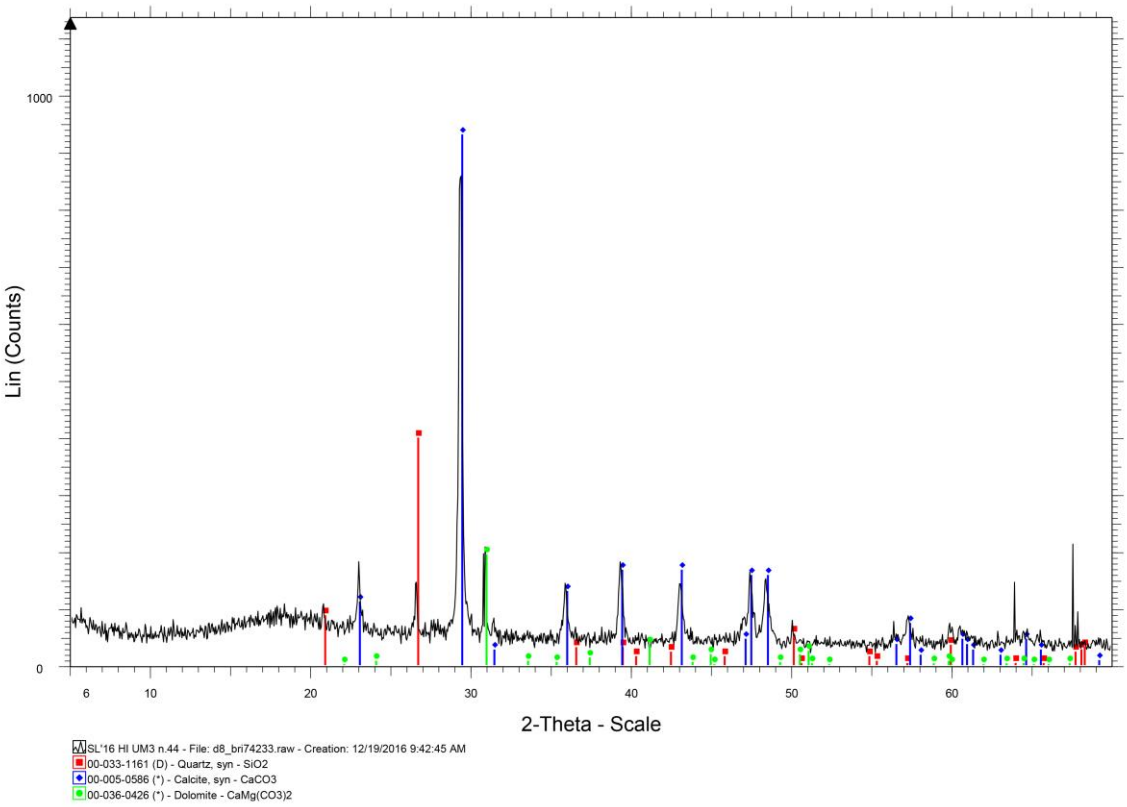

Figure 16. XRD patterns for the categories of association of crystalline phases as detected by XRD of mortar type 1 (Soto, 2017, p. 14, fig. 3)

For type 2 (Fig. 17), the binder is defined as micrite (1–4 μm) or microsparitic calcite, or a combination of both, in proportions of 60–70% with respect to the total sample. Aggregates include sub-rounded or subangular detrital quartz and fragments of sparitic limestone, both in proportions of 2–5%. Smaller amounts of red sandstone, crushed ceramics, plants and hematite (1–5%) are present. Some of the samples of this group show vuggy porosities (1mm) in proportions of 10–20%. The porosity of the mortars decreased in time due to the process of carbonation, as a secondary calcite gradually filled the pores. Interestingly, in experiments carried out with lime mortar prepared in the laboratory, the strongest specimens were the ones with the highest porosity because this characteristic allows a faster and more complete carbonation (Vyšvařil, et al., 2017). The XRD indicates the presence of quartz and calcite as the main mineralogical components in the preparation of this mortar (Fig. 18).

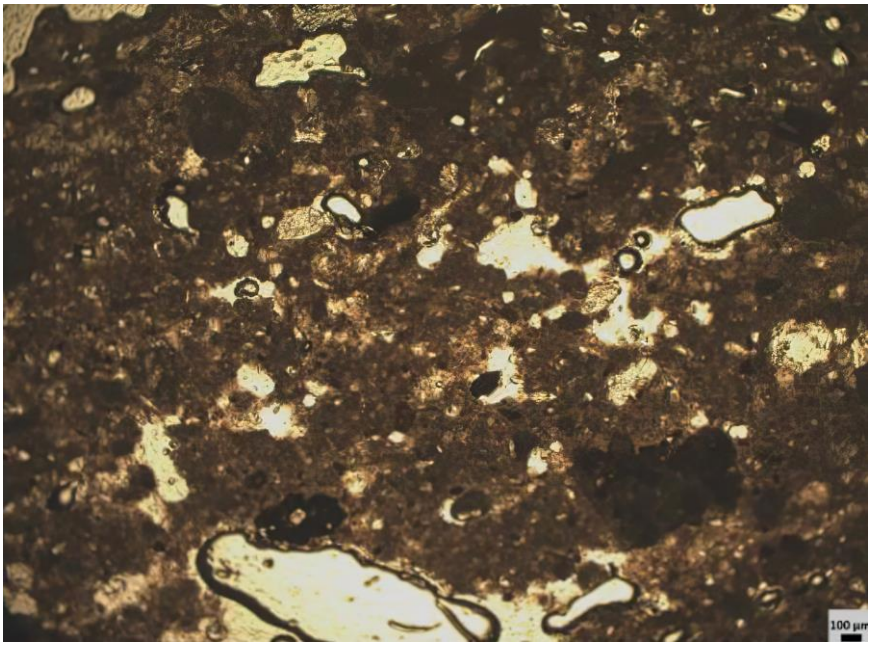

Figure 17. Optical micrograph of the thin section of lime mortar type 2. The image in plane polarized light shows vuggy porosities in the lime binder matrix (Soto, 2017, p. 25, fig. 20.2.)

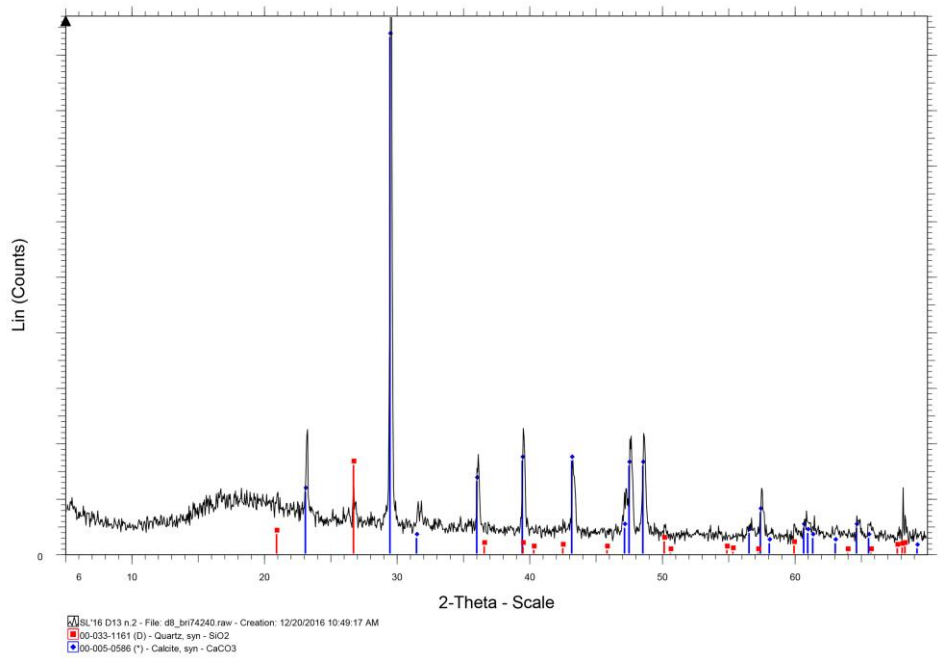

Figure 18. XRD patterns for the categories of association of crystalline phases as detected by XRD of mortar type 2 (Soto, 2017, p. 25, fig. 21)

The mortar binder in type 3 (Fig. 19) is mostly micrite, in amounts of 70–80%. The main aggregates are subangular detrital quartz (5-10%) and microsparitic limestone fragments (2–5%), and, to a lesser extent, rock with biomicritic texture (composed of bioclasts and micritic matrix), plant remains, ashes, massive hematite, and fragments of crushed ceramics. Some samples show fissures, probably related to drying processes. In this case, the binder/aggregate ratio is 3/1. The XRD of this mortar confirms quartz and calcite as the dominant minerals in the preparation (Fig. 20).

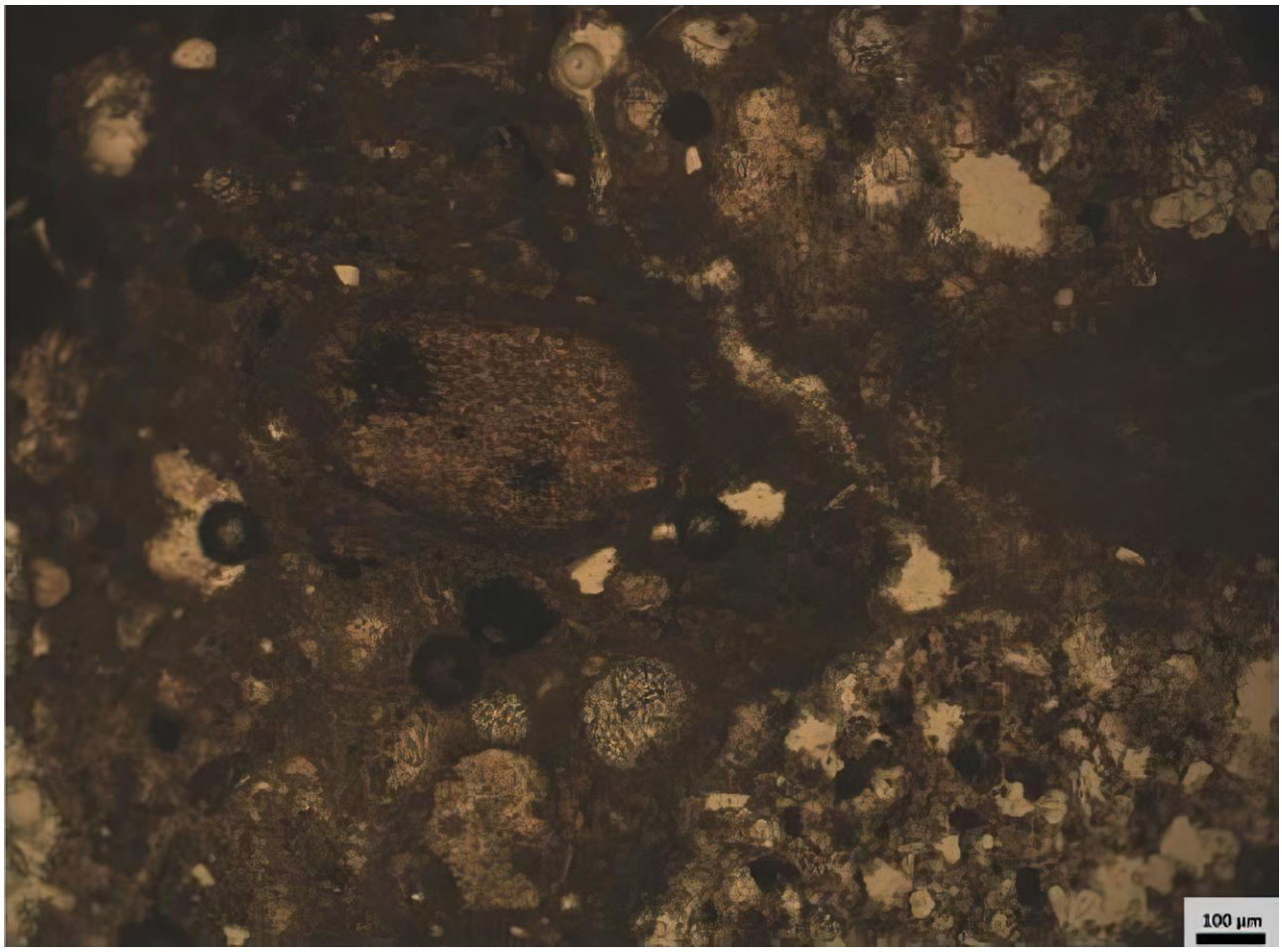

Figure 19. Optical micrograph of the thin section of the lime mortar type 2. The image in plane polarized light shows intraclasts in the lime binder matrix (Soto, 2017, p. 37, fig. 40.2)

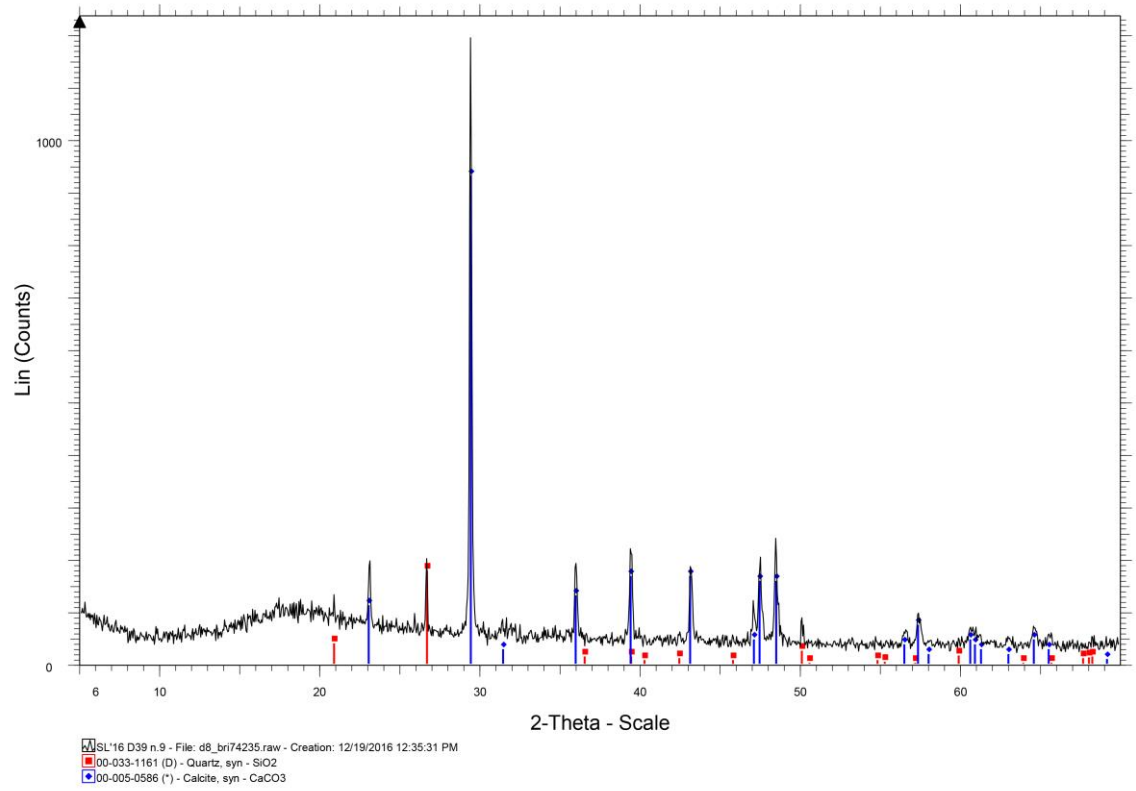

Figure 20. XRD patterns for the categories of association of crystalline phases as detected by XRD of mortar type 3 (Soto, 2017, p. 38, fig. 41)

Finally, for types 4 (Fig. 21) and 5 (Fig. 22) the binder consists of microsparitic calcite in proportions of 50-60% with respect to the total sample, and the main aggregates are fragments of microsparitic limestone and sub-rounded detrital quartz (10-30%). The main differences are in the additional aggregates, plant remains (2–5%), fragments of crushed ceramics, carbon and ashes in proportions that vary between 2% and 5% in the only sample of type 4; and fragments of gastropods, gypsum and ashes in variable portions of 1–5% are visible for type 5. The proportion of binder in these two types is lower than in the total sample of the mortars studied and seems to be a third different recipe used for the preparation of the mortars analysed in this study. Diffractograms of these two types show quartz and calcite as the dominant mineralogical components of mortar type 4 (Fig. 23) and also dolomite in the case of type 5 (Fig. 24).

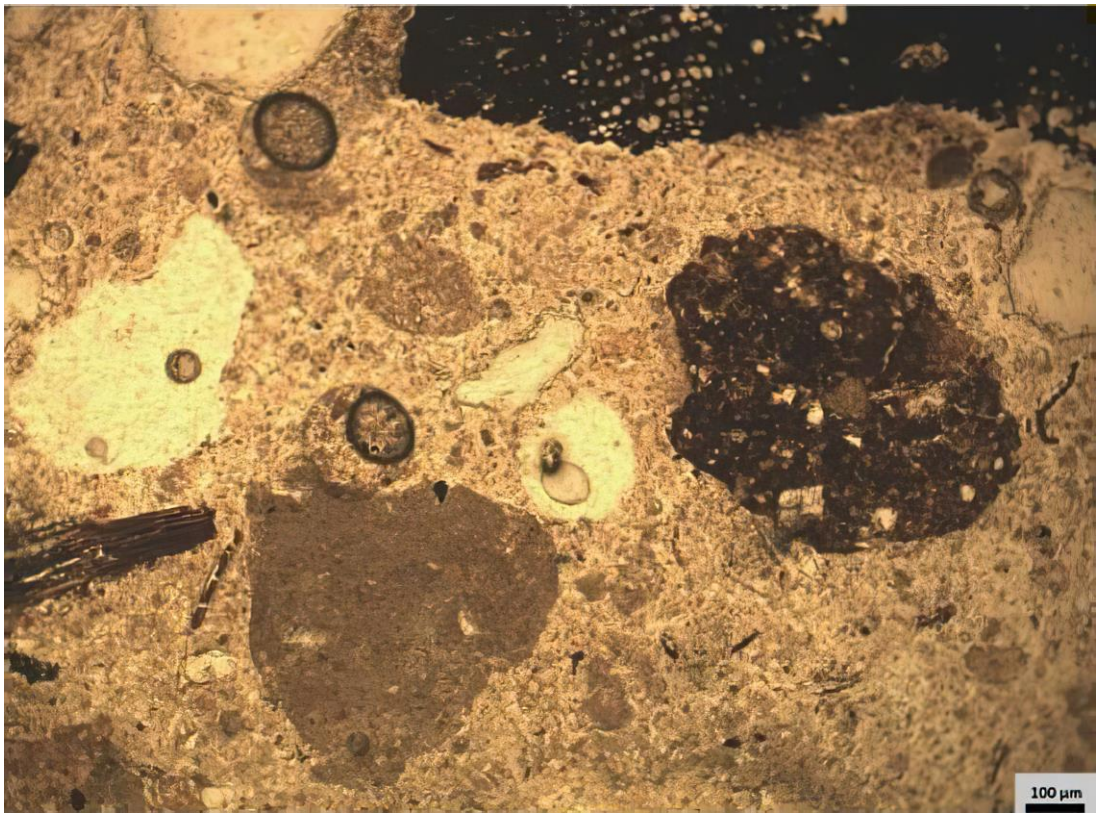

Figure 21. Optical micrograph of the thin section of the lime mortar type 4. The image in plane polarized light shows quartz and limestone as aggregates in the lime binder matrix (Soto, 2017, p. 39, fig. 43.1.)

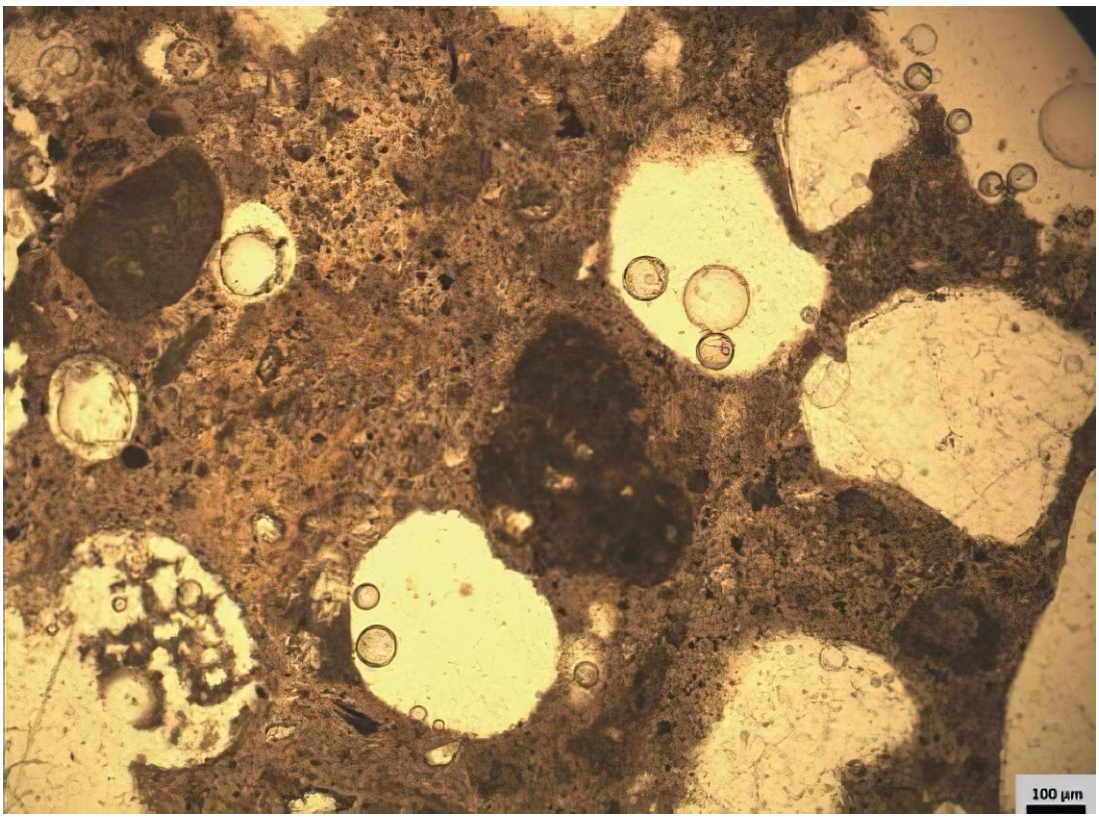

Figure 22. Optical micrograph of the thin section of lime mortar type 5. The image in plane polarized light shows quartz and limestone as aggregates in the lime binder matrix (Soto, 2017, p. 39, fig. 45.3)

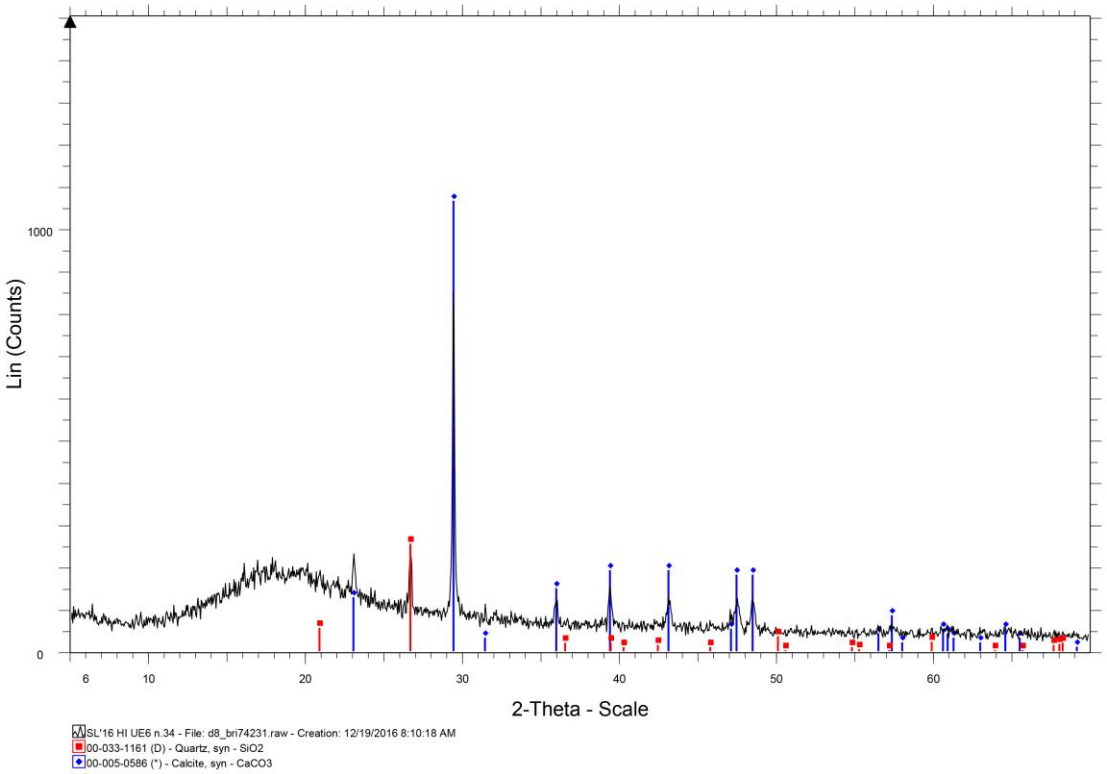

Figure 23. XRD patterns for the categories of association of crystalline phases as detected by XRD of mortar type 4 (Soto, 2017, p. 40, fig. 44)

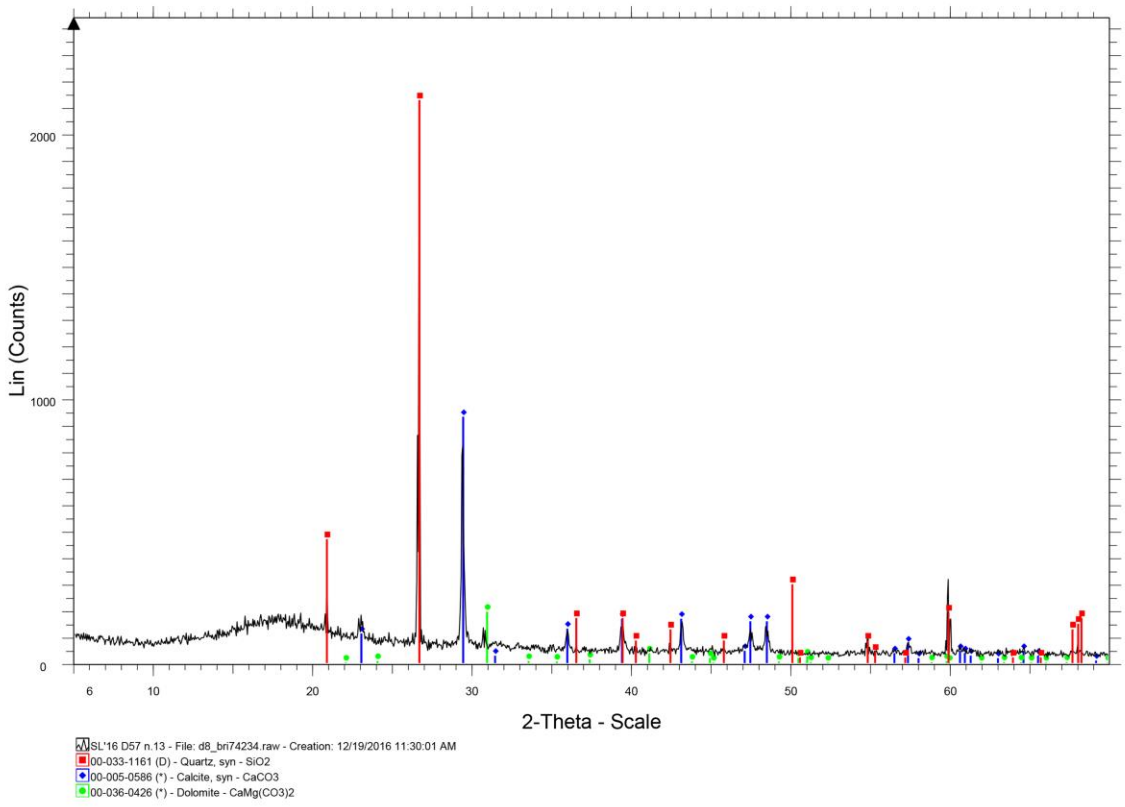

Figure 24. XRD patterns for the categories of association of crystalline phases as detected by XRD of mortar type 5 (Soto, 2017, p. 41, fig. 46)

5.2. *Mortar Radiocarbon Dating*

We are well aware of the difficulties presented by the methods currently used to date mortars (Hayen et al., 2017; Hajdas et al., 2017; Urbanova et al., 2020). Despite all the problems posed by the dates obtained, and the conviction that they do not provide us with a reliable absolute chronology of the mortars, we believe it is necessary to offer the most complete analysis possible. In this article we present new chronological data in the hope that future techniques will make it possible to obtain a wholly reliable absolute dating.

The idea behind the radiocarbon dating of mortars is clear: immediately after the preparation of mortar a chemical reaction begins in which the $Ca(OH)_2$ of the mortar reacts with CO_2 from the atmosphere to produce calcium carbonate ($CaCO_3$), creating a hard and durable binder. During this hardening process, the mortar fixes carbon from the atmosphere in its structure, and a radiocarbon signal is thus automatically created which is related to the time of building. Unfortunately, despite the efforts of researchers, mortar is still among the most difficult materials for radiocarbon dating to assess, due to its complex composition and certain other phenomena that can affect its radiocarbon content. The first problem appears when the hardening process takes years or even decades to finish, a situation which disrupts the assumed temporal association with the time the structure was built (Hale et al., 2003). A second problem appears due to the interaction of the structure with water; this may lead to the presence of deposits of carbonate transported by the water and very likely unrelated to the carbonate originally present in the structure. As a consequence, this may alter the age of the mortar. Another issue arises from the possible calcination remains coming from the original limestone, which has no radiocarbon at all. Finally, it is very common to find more geological carbonate in the aggregates used in the production, thus adding a new problem to the system (Marzaioli et al., 2013; Lubritto et al., 2015).

For all these reasons, extreme care must be taken when using mortar as a radiocarbon sample. A thorough mineralogical and petrographic characterization of the samples is essential prior to the specific treatment for radiocarbon dating. At present there are two main strategies for treating and dating mortar: sequential acid dissolution and forced suspension-based methods, including the Cryo2Sonic method (Hayen et al., 2017). Both try to separate the anthropogenic carbonate generated during the hardening of the lime mortar from other sources of carbon which are in fact contaminants: residual carbonate from incomplete combustion of the primitive lime, and carbonates added as aggregates. The first option assumes that the anthropogenic carbonate reacts faster to acid than the rock carbonates (Van Strydonck et al., 1986). Several fractions of carbon dioxide are analysed from the same mortar sample and the results are used in combination in order to obtain the age of the mortar (Hajdas et al., 2017). The second option treats the sample by repeatedly freezing and thawing, and then grinding, and sieving to separate the anthropogenic fraction and then perform a single radiocarbon analysis (Nawrocka et al., 2005).

The mortars in this study were prepared and measured at CNA (*Centro Nacional de Aceleradores*) in two different batches. The first batch comprised samples CNA4189–4193 and was prepared before the Cryo2Sonic method was first introduced at the CNA lab. These mortars were prepared using a standard carbonate sample preparation procedure as follows: after visual inspection, a small aliquot was taken and a soft leaching with HCl was applied to eliminate the outer part of the sample, which is more likely to be affected by external carbonates or recrystallization processes. Then, about 15 mg of carbonate material was used for graphitization with a CHS-AGE system (Wacker et al.(2), 2010; Wacker et al., 2013). The second batch comprised samples CNA4391–4397 and was prepared by the suspension-based method.

Cryo2Sonic is the best known version of the suspension-based method (Marzaioli et al., 2013; Addis et al., 2019). Briefly, the mortar is sequentially introduced in liquid nitrogen for five minutes and on a stove at 80ºC, also for five minutes. The cycle is repeated three times to make the mortar brittle and easy to break. The sample is then wet sieved to select fine grain under 500 μm and the material is allowed to settle until complete sedimentation.

Then, the sample is ultrasonicated for 30 minutes and the resuspended material is collected by siphoning and discarded. After the addition of more water, the rest of the material is again allowed to settle, and the material resuspended in a second ultrasonication is selected, centrifuged, and dried. The carbonate fraction selected is then graphitized in a CHS-AGE system. In both batches, about 15 mg of the carbonate is dissolved in phosphoric acid and the carbon dioxide produced is transferred to the reactors of the AGE system, where it is transformed into graphite, which is then pressed in a sample holder and is ready for AMS measurement in the Micadas system at CNA (Synal et al., 2007).

AMS targets are analysed in a batch containing unknown samples, standard samples for normalization, and blank samples for background correction. Both standard and blank samples are used to correct the AMS measurement of unknown samples, since AMS does not directly give the nominal value of the samples. In the AMS measurement the concentrations of

the three carbon isotopes, ^{12}C and ^{13}C, which are stable, and ^{14}C, which is radioactive, are determined, since all of them are needed to obtain the age of the sample. The final analysis of the data is performed using the BATS tool (Wacker et al., 2010(1)) to obtain the final Radiocarbon Ages and $\delta^{13}C$ values, which are also measured in the AMS system. The $\delta^{13}C$ parameter indicates the relative concentration of the stable isotopes and is used to correct the fact that different coetaneous materials contain slightly different radiocarbon concentrations. $\delta^{13}C$ is included in the calculation of the Radiocarbon Age, which is performed as defined by Stuiver and Polach (Stuiver and Polach, 1977), and is the experimental result of the dating process. It is expressed in years BP (Before Present) and is defined under several assumptions which are known not to be true; thus, the Radiocarbon Age does not express a real calendar age. The main assumption is that the atmospheric radiocarbon concentration has remained constant at a specific value through history.

In order to transform the Radiocarbon Age into a calendar age it is necessary to carry out a calibration procedure. This consists essentially of a comparison of the Radiocarbon Age obtained for the sample with the values of the Radiocarbon Age of a set of samples with a known calendar age (e.g., tree rings independently dated by dendrochronology), which form the calibration curve. The calibration procedure can be performed using several free access software programs; here we used CALIB software (Stuiver and Reimer, 1993) with the IntCal13 calibration curve (Reimer et al., 2013). Calibration is performed at the standard level of 2σ (95.4% confidence level). The calibration result is a set of age ranges and the probability that the real calendar age of the sample belongs to each specific range. Calibrated ranges should always be used to follow the archaeological analysis.

The results are shown in table 2. For each sample a unique lab code (CNA#) is assigned identifying the sample through the process in the laboratory. Radiocarbon age and $\delta^{13}C$ are presented as the values obtained from the AMS measurement and the following data analysis. Calibrated results are presented as the whole set of age ranges with their probability given by the calibration software (Millard, 2014). The data are presented in chronological order to simplify the archaeological analysis. A grey background is used for the first batch of samples which were prepared following a simple carbonate pretreatment. Fig. 25 presents the probability distributions of the calibrated ages for the twelve samples graphically to provide a schematic view of the historical periods obtained in the results.

Table 2. Results of Mortar Radiocarbon Dating in chronological order. Samples with a grey background belong to the first batch of samples in which a standard carbonate pretreatment was applied. The Cryo2Sonic procedure was applied to the rest of the samples. $\delta^{13}C$ values in the table were obtained from the AMS measurement.

CNA#	User Code	Age BP	$\delta^{13}C$	Calibrated ranges
4192.1.1	SL16.D16.2	3 150±30	-11.5	1498–1382 BC (*90.0%*) 1340–1310 BC (*10.0%*)
4191.1.1	SL16.D38.9	2 980±30	-8.7	1371–1359 BC (*1.2%*) 1297–1113 BC (*98.8%*)
4393.1.1	SL16.D03.5	2 890±30	-4.6	1192–1170 BC (*3.3%*) 1165–1144 BC (*3.3%*) 1131–977 BC (*93.4%*)
4193.1.1	SL16.D107.13	2 660±30	-12.2	895–868 BC (*8.7%*) 857–854 BC (*0.6%*) 850–794 BC (*90.7%*)
4394.1.1	SL16.D57.10	2 650±30	-9.6	894–870 BC (*6.3%*) 849–792 BC (*93.7%*)
4392.1.1	SL16.D22.8	2 500±30	-13.0	787–699 BC (*27.9%*) 696–540 BC (*72.1%*)
4396.1.1	SL16.D09.6	2 300±30	-6.5	404–356 BC (*82.1%*) 286–235 BC (*17.9%*)
4395.1.1	SL16.D59.11	1 260±25	-8.1	670–778 AD (*92.9%*) 791–805 AD (*2.1%*) 812–826 AD (*1.7%*) 840–862 AD (*3.3%*)
4391.1.1	SL16.H1.UM3.2 (D115)	1 000±30	-18.1	983–1049 AD (*82.2%*) 1086–1124 AD (*14.5%*) 1137–1150 AD (*3.3%*)
4189.1.1	SL16.H1.UM3.1 (D115)	980±30	-21.1	993–1055 AD (*51.0%*) 1077–1153 AD (*49.0%*)
4190.1.1	SL16.H1.6.169	970±30	-21.7	1018–1059 AD (*36.3%*)

				1065–1154 AD (*63.7%*)
4397.1.1	SL16.D13.1	910±25	-12.7	1035–1189 AD (*99.1%*) 1199–1202 AD (*0.9%*)

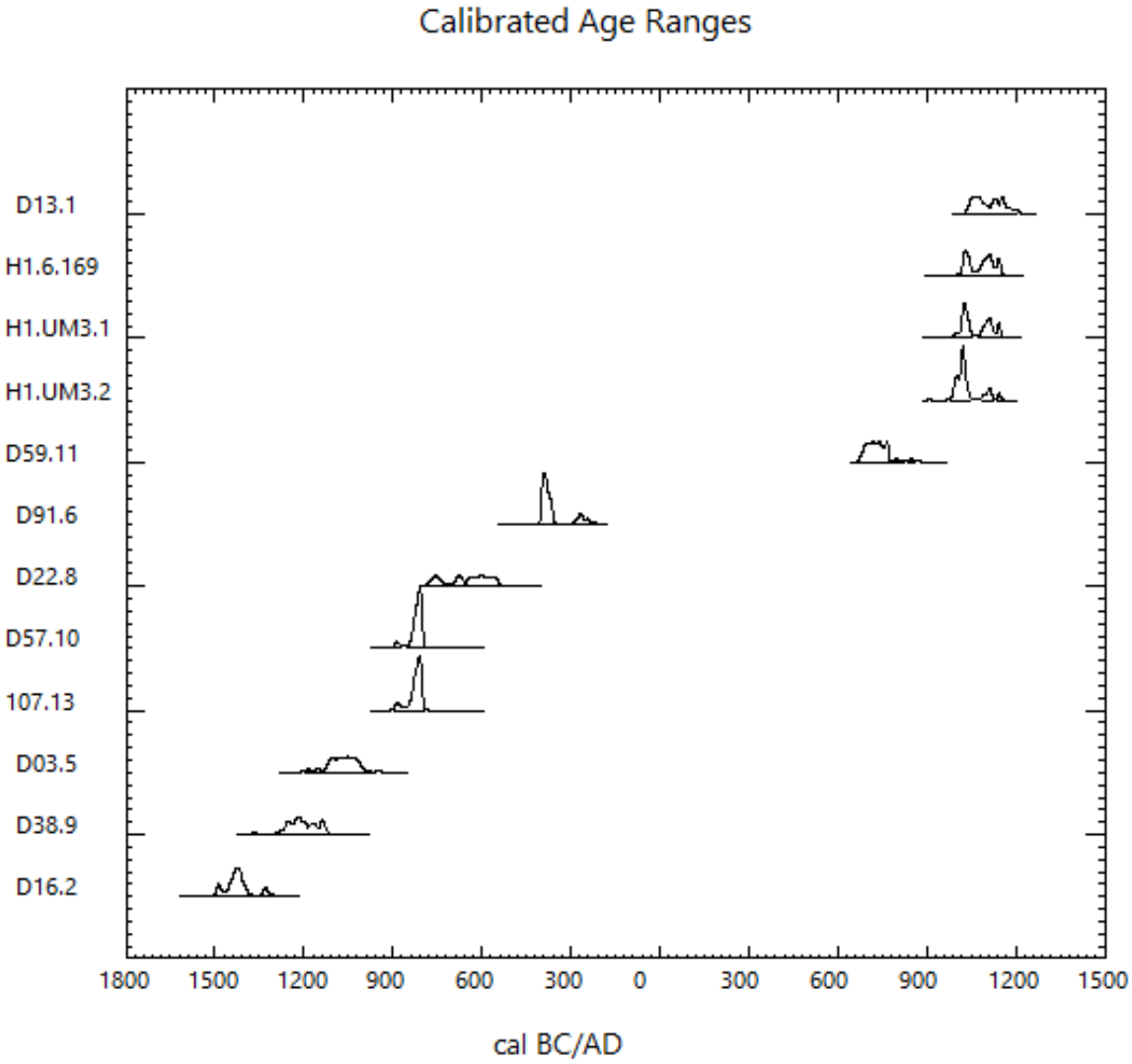

Figure 25. Calibrated age ranges at the 2σ confidence level. Names of the samples have been shortened for convenience, eliminating the common SL16. part of the original user codes.

Table 3. Combined results of the archaeological, petrographic, mineralogical and radiocarbon analyses

Sample CNA#	Hydraulic structure	Type of mortar	Type of structure	Chronology	Area of Sela
4391.1.1	H1.UM3.2 (D115)	1	Indeterminate (tank?)	X-XII centuries AD	F
4189.1.1	H1.UM3.1 (D115; re-form)	1	Indeterminate (tank?)	X-XII centuries AD	F
4190.1.1	H1.6.169	4	Indeterminate (floor?)	XI-XII centuries AD	F
4397.1.1	D13	3	Cistern with circular opening	X-XIII centuries AD	F
4192.1.1	D16	2	Cistern with oval shape	XV-XIV centuries BC	G

4393.1.1	D03	2	Cistern with oval shape	XII-X centuries BC	G
4396.1.1	D09	2	Cistern with oval shape	V-III centuries BC	G
4193.1.1	D107	5	Indeterminate (pool?)	IX-VIII centuries BC	H
4392.1.1	D22	3	Cistern with irregular shape	VIII-VI centuries BC	H
4191.1.1	D38	3	Cistern with oval shape	XIV-XII centuries BC	K
4394.1.1	D57	2	Cistern with oval shape	IX-VIII centuries BC	L
4395.1.1	D59	3	Cistern with oval shape	VII-IX centuries AD	L

6. DISCUSSION

As can be seen in Tables 2 and 3, some results coincide chronologically with various periods that are represented by the surface material, and so they can be considered plausible. Types 1 and 4 are only documented in mortars dated between the X and the XII centuries AD, type 2 in mortars dated XV-III centuries BC, type 3 in XIV-VI centuries BC and VII-XIII centuries AD, and type 5 in IX-VIII centuries BC.

These are dates in which Sela was occupied, judging by the type of surface pottery found: 4189-4190, 4193, 4391-92, 4394-4397. Some dates cluster around the XI-VI centuries BC (4192-4394, 4393, all of them corresponding to mortar type 2); there is another slightly more recent group in V-III centuries BC (4396, corresponding also to type 2, which is not found in mortars from other periods), and a third group can be dated between the VII and the XIII centuries AD (4189-90, 4391, 4395 and 4397, corresponding to mortar types 1, 4, 1, 3 and 3 respectively). Note that samples 4189 and 4391 coincide chronologically as well as in terms of the type of mortar (type 1), and both belong to the indeterminate hydraulic structure D115, which was excavated at House 1 during the 2016 campaign. Interestingly, mortar sample 4391, slightly more recent than 4189, belongs to a reform that was carried out in structure D115. Sample 4189 was obtained using the standard carbonate sample preparation procedure, and 4391 by Cryo2Sonic. From the same house sample 4190 was obtained, corresponding to mortar type 4, , and this was also analysed using the simple method[5]. Three results (4191-92, 4393, corresponding to mortar types 2 and 3) range between the XV and the XII centuries BC, so they are older than the oldest pottery documented on the surface of the site. In our opinion it is unlikely that Sela was occupied permanently in the Late Bronze age; if it had been occupied one would expect to find surface materials such as ceramics, but there are none.

As for the methods used, the simple method (the standard carbonate sample preparation procedure) which is shaded in grey in Table 1, gives two unlikely and three likely results, whereas all the results obtained by Cryo2Sonic are more or less likely. This is in agreement with our current knowledge and sample preparation techniques in mortar dating, in which very specific preparation methods are used.

Concerning the types, the differences observed especially in the binder/aggregate ratio suggest the use of at least three different recipes for the production of the lime-based mortars: one in which the binder represents 70–80% of the total sample (type 1 and 3); a second one in which it represents 60–70% (type 2); and a third one in which it accounts for approximately half (types 4 and 5). Moreover, intragroup variations are also observed. All the mortars show aggregates that would increase consistency and strength, such as crushed ceramics, ash and plants. These differences may be due to the techniques used by the various artisans or to the chronological differences indicated by radiocarbon dating.

To sum up, even if the dates obtained are not totally unreasonable, what is in doubt here is the reliability of the currently available methods for dating mortars, which determine the results. An additional problem is that we lack independent chronological indications for dating the mortars or cisterns in Sela, such as morphology, type of manufacture, etc., able to confirm or refute the results obtained. For example, sample CN4392 from cistern D22 is dated between the VIII-VI centuries BC, which is in full agreement with, for example, the evidence from the Nabonidus inscription. But we lack an independent date for D22. In our opinion, all these data need to be confirmed in the

[5] Note that these dates are noticeably older than the 14C dates of the wood samples taken from House 1, for which the following absolute chronologies were obtained: sample CNA4194.1.1. from Layer 5 (Cal AD 1643-1682); sample CNA4195.1.1. from Layer 6 (Cal AD 1486-1604); and sample CNA4196.1.1. from Layer 10 (Cal AD 1451-1529), see Da Riva et al., forthcoming. But we stress that wood samples can also be problematic, as this material is often intrusive.

future by further archaeological research at the site and more mineralogical, petrographic and AMS radiocarbon analyses in order to obtain supplementary evidence that may corroborate or modify the results presented here.

7. CONCLUSION

As-Sila/Sela is a site in the area of at-Tafilah with a remarkably rich archaeological legacy and an imposing geomorphological heritage (Figs 26-29). Its extension, the presence of many architectural structures, the surface finds, and its general layout bear witness to its enormous archaeological potential. The many structures for water storage and management, as well as the dwellings and fortifications, make it a unique site for studying the economic and social relevance of water management on the Edomite Plateau. With the information provided by the archaeological surveys and excavations (Da Riva et al., 2017; Da Riva et al., forthcoming), we can now affirm that as-Sila was indeed occupied during the Late Iron Age, in the Nabataean and Roman periods, and also in Mamluk and Ottoman periods (12th–18th centuries AD). The topographic study and preliminary survey demonstrate the enormous potential of the site for contributing to the understanding of the past on the Edomite Plateau and for helping us to solve questions regarding settlement patterns, water control systems, and economic activity. Regarding water management, the amount, and the variety, of elements of hydraulic control present in Sela is astonishing. For this reason, detailed investigations have been carried out in the structures of the site, including the studies of the mortars presented here.

Figure 26. General view of area K. Photo by Matthew Dalton APAAME 20181014 MND-0537©APAAME

Figure 27. Cisterns in area H. Photo by Robert Bewley APAAME 20181014 RHB-0382©APAAME

Figure 28. Entrance gate and tower with cistern(?) D10 area F. Photo by Matthew Dalton APAAME 20181014 MND-0542©APAAME

Figure 29. View of Sela from the East, stairway can be seen to the right. Photo by Mathew Dalton APAAME 20181014 MND-0574©APAAME

The results of petrographic and mineralogical analyses of the mortars show that they are all lime-based and were mixed with aggregates to increase their consistency and strength. The differences observed in the binder/aggregate ratio suggest the use of at least three different recipes that might suggest the involvement of diverse artisans, possibly in different periods. Despite their diversity, the mortars show the characteristics required to fulfil their function of protecting and waterproofing the hydraulic structures of the water system of Sela. The proximity of quarries of limestone and sandstone would have allowed access to the main raw materials needed for the production of the mortars. Their production involved a well-standardized process and required large quantities of combustible and the participation of skilled artisans; clearly, in view of the large number of water structures identified at the site, mortar production would have been an important activity. Although no stable structures have been found, rudimentary kilns of some sort must have been used for the calcination process.

As demonstrated in this article, mortar is still one of the most difficult materials for radiocarbon dating to assess, and the results obtained should be taken with a grain of salt. However, in spite of all the problems posed by the dates presented above, and even though we know that they do not provide us with an absolute chronology, we believe it is worthwhile to present them here so as to offer the most complete analysis of the mortars from Sela currently available.

ACKNOWLEDGEMENTS

We thank the anonymous reviewers for their constructive comments. The Sela Archaeological Project, led by R. Da Riva of the University of Barcelona (UB) in collaboration with the Department of Antiquities of Jordan (DoAJ), has been funded by the ICREA Academia Research Award, the Spanish Ministry of Education and Culture, the Agència de Gestió d'Ajuts Universitaris i de Recerca, AGAUR, of the Autonomous Government of Catalonia, and the PALARQ Foundation. The project also has the support of the Spanish Embassy in Amman. Except where otherwise noted, all photographs and materials published here are ©Sela Archaeological Project. The authors would especially like to thank Bob Bewley and Matthew Dalton of The Aerial Archaeology in Jordan Project for allowing us to use the aerial images taken in Sela in October 2018 (©APAAME). We

would also like to thank María Soto and Josep Vallverdú who made the petrographic and mineralogical analyses at the IPHES and who most kindly put this information at our disposal. These analyses, as well as the ^{14}C analysis at the CNA were financed by research grants of the PALARQ Foundation to which the authors express their most sincere gratitude.

REFERENCES

Addis, A., Secco M., Marzaioli, F., Artioli, G., Chavarría Arnau, A., Passariello, I., Terrasi, F. and Brogiolo, J. P. (2019) Selecting the Most Reliable 14C Dating Material Inside Mortars: The Origin of the Padua Cathedral. *Radiocarbon*, Vol. 61, pp. 375-393.

Al-Aseer, R. (2000) Chemical Analysis of Nabatean Dam Mortar in Petra. MA Thesis, Yarmouk University.

Al Sekhaneh, W., Shiyyab, A., Arinat, M., Gharaibeh, N. (2020) Use of FTIR and thermogravimetric analysis of ancient mortar from The Church of the Cross in Gerasa (Jordan) for conservation purposes. *Mediterranean Archaeology and Archaeometry* Vol. 20 (3), pp. 159-17.

Artioli, G., Secco, M. and Addis, A. (2019) The Vitruvian legacy: mortars and binders before and after the Roman world. *EMU Notes in Mineralogy*, Vol. 20, pp. 151-202.

Benedetto, C Di, Graziano, S.F, Guarino, V, Rispoli, C, Munzi, P, Morra, V, Cappelletti, P (2018) Romans' established skills: mortars from d46b mausoleum, porta mediana necropolis, Cuma (Naples). *Mediterranean Archaeology and Archaeometry,* Vol. 18, No 5, pp. 131-146. DOI: 10.5281/zenodo.1285895

Ben David, Ch. (2015) You who live in the clefts of the rocks' (jer.49:16): Edomite mountain strongholds in southern Jordan. ARAM 27, 227-238.

Brysbaert, A. (2007) Murex uses in plaster features in the Aegean and eastern Mediterranean Bronze Age. *Mediterranean Archaeology and Archaeometry*, Vol. 7, pp. 29-51.

Buxeda i Garrigós, J. and Madrid i Fernández, M. (2016) Designing Rigorous Research: Integrating Science and Archaeology. In *The Oxford Handbook of Archaeological Ceramic Analysis*, A. Hunt (ed.), Oxford, Oxford University Press, pp. 19-47.

Da Riva, R. (2019) The King of the Rock Revisited: the site of as-Sila (Tafila, Jordan) and the inscription of Nabonidus of Babylon. In *Over the Mountains and Far Away. Studies in Ancient Near Eastern History and Archaeology presented to Mirjo Salvini on the Occasion of His 80th Birthday*, P. S. Avetisyan, R. Dan, and Y. H. Grekyan (ed.), Oxford, Archaeopress, pp. 161-174.

Da Riva, R. (2020) The Nabonidus Inscription in Sela (Jordan): epigraphic study and historical meaning. *Zeitschrift für Assyriologie und Vorderasiatische Archäologie*, Vol. 110, No. 2, pp. 176-195.

Da Riva, R., Muñiz, J., Corrada, M., Jariri, Eh., Gaspar, D., Madrid, M., and Marsal, R. (2017), An Archaeological Survey of the Site of as-Silaʿ/Selaʿ (Tafila), *Annual of the Department of Antiquities of Jordan*, Vol. 58, pp. 623-640.

Da Riva R., Marsal, R., Madrid, M., Miguel, E., Marín, J., Allué, E., and Lozano, M. (forthcoming) The site of Sela: Archaeological Campaign 2016, *Annual of the Department of Antiquities of Jordan*, Vol. 60, pp. xx-xx.

Degryse, P., Elsen, J. and Waelkens, M. (2002) Study of ancient mortars from Sagalassos (Turkey) in view of their conservation. *Cement and Concrete Research*, Vol. 32, pp. 1457-1463.

Gourdin, W. H. and Kingery, W. D. (1975) The Beginnings of Pyrotechnology: Neolithic and Egyptian Lime Plaster. *JAF*, Vol. 2, pp. 133-150.

Hale, J., Heinemeier, J., Lancaster, L., Lindroos, A. and Ringbom, Å. (2003) Dating Ancient Mortar. *American Scientist*, Vol. 91, pp. 130-137.

Hajdas, I., Lindroos, A., Heinemeier, J., Ringbom, Å., Marzaioli, F., Terrasi, F., Passariello, I., Capano, M., Artioli, G., Addis, A., Secco, M., Michalska, D., Czernik, J., Goslar, T., Hayen, R., Van Strydonck, M. Fontaine, L., Boudin, M., Maspero, F., Panzeri, L., Galli, A., Urbanová, P., and Guibert, P. (2017) Preparation and Dating of Mortar Samples – Mortar Dating Inter-Comparison Study (MODIS). *Radiocarbon*, Vol. 59, No. 6, pp. 1845-1858.

Hauptmann, A. and Ünsal, Y. (2001) Lime Plaster, Cement and the First Puzzolanic Reaction. *Paléorient*, Vol. 26, pp. 61-68.

Hayen, R., Van Strydonck, M., Fontaine, L., Boudin, M., Lindroos, A., Heinemeier, J., Ringbom, Å., Michalska, D., Hajdas, I., Hueglin, S., Marzaioli, F., Terrassi, F., Pasariello, I., Capano, M., Maspero, F., Panzeri, L., Galli, A., Artioli, G., Addis, A., Secco, M., Boaretto, E., Moreau, Ch., Guibert, P., Urbanova, P., Czernik, J., Goslar, T., and Caroselli, M. (2017) Mortar Dating Methodology: Assessing Recurrent Issues and needs for Further Research. *Radiocarbon*, Vol. 59, pp. 1859-1871.

Hobbs, L. W. and Siddall, R. (2011) Cementitious materials of the ancient world. In Building Roma Aeterna: Current Research on Roman Mortar and Concrete, *Proceedings of the Conference, March 27-29, 2008 (Commentationes Humanarum Litterarum, 128)*, Å. Ringbom, R. L. Hohlfelder, Sjöberg, P., and Sonck-Koota, P. (ed.), Helsinki, Societas Scientiarum Fennica, pp. 35-60.

Kingery, W. D., Vandiver, P. B. and Prickett, M. (1998) The Beginnings of Pyrotechnology, Part II: production and use of Lime and Gypsum plaster in the Pre-Pottery Neolithic Near East. *Journal of Field Archaeology*, Vol. 15, pp. 219-244.

Lindner, M. (1992) Edom outside the famous excavations: Evidence from surveys in *the greater Petra area, In Early Edom and Moab: The beginning of the Iron Age in southern Jordan*, P. Bienkowski (ed.), Sheffield, Equinox, pp. 143-166.

Lindner, M. and S. Farajat (1987) An Edomite mountain stronghold north of Petra (Ba'ja III). *Annual of the Department of Antiquities of Jordan*, Vol. 31, pp. 175-185.

Lindner, M., Hübner, U., Gunsam, E. (2001) Es-Sela, 2500 Jahre Fliehburg und Bergfestung in Edom, *Sudjordanien. Das Altertum*, Vol. 46, pp. 243-278.

Lubritto, C., Caroselli, M., Lugli, S., Marzaioili, F., Nonni, S., Marchetti Dori, S. and Terrassi, F. (2015) AMS Radiocarbon Dating of Mortar: The Case Study of the Medieval UNESCO site of Modena. Nuclear Instruments and Methods in *Physics Research Section B*, Vol. 361, pp. 614-619.

MacDonald, B. (2015) *The southern Transjordan Edomite plateau and the Dead Sea rift valley. The Bronze Age to the Islamic period (3800/3700 BC–AD 1917)*. Oxford, Oxbow Books.

MacDonald, B., Herr, L. G., Neeley, M. P., Gagos, T., Moumani, K., Rockman, M. (2004) *The Tafila-Busayra Archaeological Survey 1999-2001, West-Central Jordan*, Boston, American Schools of Oriental Research.

Marzaioli, F., Nonni, S., Passariello, I., Capano, M., Ricci, P., Lubritto, C., De Cesare, N., Eramo, G., Quirós Castillo, J. A. and Terrassi, F. (2013) Accelerator Mass Spectrometry 14C Dating of Lime Mortars: Methodological Aspects and Field Study Applications at CIRCE (Italy). Nuclear Instruments and Methods in *Physics Research B*, Vol. 294, pp. 246-251.

Millard, A. R. (2014) Conventions for Reporting Radiocarbon Determinations. *Radiocarbon*, Vol. 56, pp. 555-559.

Nawrocka, D., Czernik, J. and Goslar, T. (2005) 14C Dating of Carbonate Mortars from Polish and Israeli sites. *Radiocarbon* ,Vol. 51, No. 2, pp. 857-866.

Pavia, S. and Caro, S. (2008) An Investigation of Roman Mortar Technology through the Petrographic Analysis of Archaeological Material. *Construction and Building Materials*, Vol. 22, pp. 1807-1811.

Pecchioni, E., Fratini, F., and Cantisani, E. (2014) *Atlas of the ancient mortars in thin section under optical microscope*. Nardini Editore, Firenze.

Porter, B. W. (2004) Authority, Polity, and tenuous Elites in Iron Age Edom (Jordan). *Oxford Journal of Archaeology*, Vol. 23, pp. 373-395.

Regev, L., Zukerman, A., Hitchcock, L., Maeir, A. M., Weiner, S. and Boaretto, E. (2010) Iron Age Hydraulic Plaster from Tell es-Safi/Gath, Israel. *Journal of Archaeological Science*, Vol. 37, pp. 3000-3009.

Reimer, P. J., Bard, E., Bayliss, A., Beck, J. W., Blackwell, P. G., Bronk Ramsey, C., Buck, C. E., Cheng, H., Edwards, R. L., Friedrich, M., Grootes, P. M., Guilderson, T. P., Haflidason, H., Hajdas, I., Hatté, C., Heaton, T. J., Hoffmann, D. L., Hogg, A. G., Hughen, K. A., Kaiser, F., Kromer, B., Manning, S. W., Niu, M., Reimer, R., Richards, D. A., Scott, E. M., Southon, J. R., Staff, R. A. S. Turney, Ch. S., and van der Plicht, J. (2013) IntCal13 and Marine13 Radiocarbon age Calibration curves 0–50,000 years cal BP. *Radiocarbon*, Vol. 55, pp. 1869-1887.

Salama,K.K, Ali, M.F, Moussa, A.M (2017) the presence of cement mortars in the added chambers of el sakakeny palace: a case study. *SCIENTIFIC CULTURE*, Vol. 3, No. 3, pp. 25-29. DOI: 10.5281/zenodo.813134.

Shqiarat Mansour (2019) History and archaeology of water management in Jordan through ages. *SCIENTIFIC CULTURE,* Vol. 5, No. 3, pp. 41-54. DOI: 10.5281/zenodo.3340109.

Soto, M. (2017) *Informe de caracterización de los morteros de las estructuras hidráulicas del yacimiento de Sela (Jordania)*. Institut Català de Paleoecologia Humana i Evolució Social (unpublished).

Synal, H.-A., Stocker, M. and Suter, M. (2007) MICADAS: A new Compact Radiocarbon AMS System. *Nuclear Instruments and Methods in Physics Research Section B: Beam Interactions with Materials and Atoms*, Vol. 59, pp. 7-13.

Stuiver, M., and Polach, H. A (1977) Reporting of 14C Data. *Radiocarbon*, Vol. 19, pp. 355-363.

Stuiver, M., and Reimer, P. J. (1993) Extended 14C Data Base and Revised CALIB3.0 14C Age Calibration Program. *Radiocarbon*, Vol. 35, pp. 215-230.

Theologitis, A, Kapridaki C, Kallithrakas-Kontos, N, Maravelaki-Kalaitzaki, P and Fotiou, A (2021) Mortar and plaster analysis as a directive to the design of compatible restoration materials in frangokastello (Crete). *Mediterranean Archaeology and Archaeometry*. Vol. 21, No 1, pp. 109-120DOI: 10.5281/zenodo.4284427

Urbanova, P., Boaretto, E. and Artioli, G. (2020) The State-of-the-Art of Dating Techniques Applied to Ancient Mortars and Binders: A Review. *Radiocarbon*, Vol. 62, pp. 503-525.

Van Strydonck, M., Dupas, M., Dauchot-Dehon, M., Pachiaudi, Ch. and Marechal, J. (1986) The Influence of Contaminating (fossil) Carbonate and the Variation of □13C in Mortar Dating. *Radiocarbon*, Vol. 28, pp. 702-710.

Vázquez-Calvo, C, Fort, R, Romero, D, Beltrán, A and Sánchez-Palencia, F.J. (2016) Roman bedrock mortars: new findings for interpreting data at the Roman pino del Oro Gold mines (Spain). *Mediterranean Archaeology and Archaeometry*, Vol. 16, No 2, pp. 139-148. DOI:10.5281/zenodo.53072

Vyšvařil, M., Žižlavský, T, and Bayer, P. (2017) "he Effect of Aggregate Type on the Properties of Lime Mortars. *Applied Mechanics and Materials*, No. 861, pp. 141-148.

Wacker, L., Christl, M. and Synal, H.-A. (2010) Bats: A new Tool for AMS Data Reduction. *Nuclear Instruments and Methods in Physics Research B*, Vol. 268, pp. 976-979.

Wacker, L., Němec, N. and Bourquin, J. (2010) A Revolutionary Graphitisation System: Fully Automated, Compact and Simple. *Nuclear Instruments and Methods in Physics Research B*, Vol. 268, pp. 931-934.

Wacker, L., Hajnalka Fülöp, R., Hajdas, I., Molnár, M. and Rethemeyer, J. (2013) A Novel Approach to process Carbonate Samples for Radiocarbon with Helium Carrier Gas. *Nuclear Instruments and Methods in Physics Research B*, Vol. 294, pp. 214-217.